Density Matrix Renormalization Group Approach for Many-Body Open Quantum Systems

J. Rotureau,[1,2,3] N. Michel,[1,2,3] W. Nazarewicz,[1,2,4] M. Płoszajczak,[5] and J. Dukelsky[6]

[1]*Department of Physics and Astronomy, University of Tennessee, Knoxville, Tennessee 37996, USA*
[2]*Physics Division, Oak Ridge National Laboratory, Oak Ridge, Tennessee 37831, USA*
[3]*Joint Institute for Heavy Ion Research, Oak Ridge National Laboratory, P.O. Box 2008, Oak Ridge, Tennessee 37831, USA*
[4]*Institute of Theoretical Physics, University of Warsaw, ul. Hoża 69, 00-681 Warsaw, Poland*
[5]*Grand Accélérateur National d'Ions Lourds (GANIL), CEA/DSM-CNRS/IN2P3, BP 55027, F-14076 Caen Cedex, France*
[6]*Instituto de Estructura de la Materia, CSIC, Serrano 123, 28006 Madrid, Spain*

(Received 3 March 2006; published 13 September 2006)

The density matrix renormalization group (DMRG) approach is extended to complex-symmetric density matrices characteristic of many-body open quantum systems. Within the continuum shell model, we investigate the interplay between many-body configuration interaction and coupling to open channels in case of the unbound nucleus ^{7}He. It is shown that the extended DMRG procedure provides a highly accurate treatment of the coupling to the nonresonant scattering continuum.

DOI: 10.1103/PhysRevLett.97.110603 PACS numbers: 05.10.Cc, 02.60.Dc, 02.70.−c, 21.60.Cs

The theoretical description of strongly correlated open quantum systems (OQS), such as the weakly bound or unbound atomic nuclei or atomic clusters, requires the rigorous treatment of both the many-body correlations and the continuum of positive-energy states and decay channels. The solution of this challenging problem has been advanced recently in the OQS formulation of the nuclear shell model (SM), the so-called Gamow shell model (GSM). GSM is the multiconfigurational SM with a single-particle (SP) basis given by the Berggren ensemble [1] consisting of Gamow (resonant or Siegert) states and the nonresonant continuum of scattering states. The resonant states are the generalized eigenstates of the time-independent Schrödinger equation, which are regular at the origin and satisfy purely outgoing boundary conditions. The SP Berggren basis is generated by a finite-depth potential, and the many-body states can be expanded in Slater determinants spanned by resonant and nonresonant SP basis states [2,3]. The use of the Berggren ensemble implies the complex-symmetric representation for the many-body Hermitian Hamilton operator, H_{GSM}. Of all the eigenstates of H_{GSM}, of major interest are the many-body resonant states representing either bound states or narrow resonances corresponding to various decaying channels [4].

The identification of the many-body resonant states is a major conceptual and numerical task. In general, many-body resonant states of GSM do not correspond to the lowest-energy eigenvalues. Instead, they are obtained in the two-step generalized Lanczos procedure. In the first step, H_{GSM} is diagonalized in a basis consisting of SP resonant states only (the pole approximation) and provides the first-order approximation to many-body resonances $|\Psi_i\rangle^{(0)}$, where index i enumerates all eigenvectors in this restricted space (the pole space). These eigenvectors have, by construction, outgoing asymptotics; they serve as pivots in the second step of the procedure where one includes couplings to nonresonant continuum states. Many-body resonant states in the full GSM space correspond to the eigenstates having the largest overlap with vectors $|\Psi_i\rangle^{(0)}$. The GSM, which up to now has been applied to weakly bound or unbound atomic nuclei [2,3,5], can be equally applied for the description of other OQS, e.g., open microwave resonators and self-bound atomic systems, such as $^3\mathrm{He}_N$ neutral droplets at the limits of their stability [6]. Another possible application of the GSM is to quantum dots, where the interplay between electron-electron correlations and the continuum coupling yields the transition in the conductance properties.

The principal limitation of GSM applications is the explosive growth in the number of configurations (i.e., dimension of the many-body Fock space) with both the number of active particles and the size of the SP space. To ensure completeness of the Berggren basis, for each resonant SP state with the angular momentum quantum numbers l and j, one should include a large set of discrete nonresonant continuum states $\{(l_j)^{(f)}; f = 1, \ldots, M\}_c$ lying on a continuous contour $L_+^{l_j}$ in the complex k plane [2,3]. These continuum states become new active shells in the many-body framework of GSM, and because of their presence, the dimension of the H_{GSM} matrix grows extremely fast, and the matrix is also significantly denser than that of a conventional SM. On the other hand, most of the configurations involving many particles in the nonresonant continuum contribute very little to low-energy GSM eigenfunctions. This means that a different strategy, based on a dominant role of the pole space in the GSM, should be developed for a smart selection of the most important configurations involving nonresonant continuum states. For that purpose, we propose a new method based on the density matrix renormalization group (DMRG) approach for finding the resonant states of H_{GSM}.

The DMRG method was introduced to overcome the limitations of Wilson-type renormalization groups to describe strongly correlated 1D lattice systems with short-

range interactions [7] (see recent reviews [8,9]). Extensions of DMRG to 2D lattice models are, in general, less accurate and require a reduction to a 1D problem by selecting a path in the 2D plane. More recently, by reformulating the DMRG in a SP basis, several applications to finite Fermi systems like molecules [10], superconducting grains [11], quantum dots [12], and atomic nuclei [13] have been reported. While most of the DMRG studies were focused on equilibrium properties in strongly correlated closed quantum systems (CQS) with Hermitian density matrix, nonequilibrium systems involving non-Hermitian and nonsymmetric density matrices can also be treated [14]. The applications of DMRG in the context of the SM (the CQS formalism), both in the M scheme [15] and in the angular-momentum-conserving J scheme [16], exhibit convergence problems. In this work, we shall present the first detailed test of the J-scheme DMRG approach [17] in the many-body OQS described by the GSM [2,3]. The main idea of the GSM + DMRG approach is to gradually consider different SP shells of the discretized nonresonant continuum in the configuration space and retain only $N_{\rm opt}$ optimal states dictated by the eigenvalues of the density matrix with the largest modulus. The procedure will be illustrated using the example of many-body resonances in the neutron-unbound nucleus ^{7}He described in terms of $N_\nu = 3$ active (valence) neutrons outside the closed (and inert) core of ^{4}He.

The SP basis is generated by a Woods-Saxon (WS) potential with the radius $R_0 = 2$ fm, the depth of the central potential $V_0 = 47$ MeV, the diffuseness $d = 0.65$ fm, and the spin-orbit strength $V_{\rm so} = 7.5$ MeV [2]. This SP potential reproduces experimental energies and widths of the SP resonances $3/2^-_1$ (g.s.) and $1/2^-_1$ (first excited state) in ^{5}He. The neutron valence space consists of the $0p_{1/2}$ and $0p_{3/2}$ resonant SP shells and the corresponding nonresonant shells $\{p_{1/2}\}_c, \{p_{3/2}\}_c$. The $L_+^{p_{1/2}}$ contour in the complex-k plane (in the following, k is expressed in units of fm^{-1}) is defined by a triangle with vertices at $[\mathrm{Re}(k), \mathrm{Im}(k)] = (0,0)$, $(0.33, -0.33)$, $(0.5, 0.0)$, and a segment along the Re(k) axis from $(0.5, 0)$ to $(1.0, 0.0)$. Similarly, $L_+^{p_{3/2}}$ is given by a triangle: $(0, 0)$, $(0.17, -0.17)$, $(0.5, 0)$, and a straight segment from $(0.5, 0)$ to $(1.0, 0)$. Each segment of these contours is discretized with the same number of points corresponding to the abscissas for the Gauss-Legendre quadrature. $H_{\rm GSM}$ is a sum of the WS potential, representing the effect of a ^{4}He core, and the two-body interaction among valence neutrons. The latter is approximated by a finite-range surface Gaussian interaction [5] with the range $\mu = 1$ fm and the coupling constants depending on the total angular momentum J of the neutron pair: $V_0^{(J=0)} = -542$ MeV fm^3, $V_0^{(J=2)} = -479$ MeV fm^3. These constants are fitted to reproduce the binding energies of ^{6}He and ^{7}He with respect to the core. Since the core is assumed to be inert, the recoil effects are ignored, and the center-of-mass always lies at the origin.

The special role of the pole space in the GSM suggests that the configuration space in GSM + DMRG applications should be divided in two subspaces: A (the pole space built from the SP resonant shells $\{0p_{1/2}, 0p_{3/2}\}$), and B (built from the SP nonresonant shells $\{p_{1/2}\}_c$ and $\{p_{3/2}\}_c$). In the warm-up phase of DMRG, we proceed as follows: (i) Construct all families $\{n; j_A\}$ of states $|k\rangle_A$ with $n = 0, 1, \ldots, N_\nu$ particles coupled to all possible j_A values. Calculate and store the matrix elements of the Hamiltonian and all suboperators in A: $\{O\} = \{a^\dagger, (a^\dagger \tilde{a})^K, (a^\dagger a^\dagger)^K, ((a^\dagger a^\dagger)^K \tilde{a})^L, ((a^\dagger a^\dagger)^K (\tilde{a}\,\tilde{a})^K)^0\}$. Diagonalize $H_{\rm GSM}$ in the pole space to obtain the first approximation $|\Psi_J\rangle^{(0)}$ for the target state. (ii) Add the first pair $(p_{1/2}, p_{3/2})_c^{(f=1)}$ of SP shells by coupling states in A with those in B, $\{|k\rangle_A |i\rangle_B\}^J$. Each resulting state has a fixed angular momentum J and total particle number N_ν. Calculate the matrix elements of $H_{\rm GSM}$ and all suboperators within this space. (iii) Diagonalize $H_{\rm GSM}$ in the enlarged space, and from all eigenstates, $|\Psi_J\rangle = \sum_{k,i} c_{ki} \{|k\rangle_A |i\rangle_B\}^J$, select the one that has the largest overlap with $|\Psi_J\rangle^{(0)}$ [18]. (iv) From this selected eigenstate calculate the reduced density matrix $\rho^B_{ii';j_B} = \sum_k c^{(j_B)}_{ki} c^{(j_B)}_{ki'}$ for each *fixed* value of j_B [19,20]. Diagonalize ρ^B, and select $N^0_{\rm opt}$ eigenstates $|\alpha\rangle_B = \sum_i d^\alpha_i |i\rangle_B$ having the largest absolute values of their eigenvalues. Recalculate and store all the matrix elements of suboperators for these optimized states: $B\langle\alpha|O|\beta\rangle_B = \sum_{i,i'} d^\alpha_i d^\beta_{i'B} \langle i|O|i'\rangle_B$. (v) Add the next pair of shells $(p_{1/2}, p_{3/2})_c^{(f=2)}$ in B following steps (ii)–(iv). (vi) Continue the procedure until the last shell $(p_{1/2}, p_{3/2})_c^{(f=N_c)}$ in B is reached.

At this point, the warm-up phase ends and the so-called sweeping phase begins. Starting from the last pair of shells in B, the process continues in the reverse direction. For instance, if the mth pair of p shells in B is reached, the Hamiltonian is diagonalized in the set of vectors: $\{(|k, i_{\rm prev}\rangle)^{J_{\rm part}} |i\rangle\}^J$, where $|i_{\rm prev}\rangle$ is a previously optimized state (constructed during the warm-up phase from first $m-1$ pairs of shells in B and coupled with $|k_A\rangle$ to $J_{\rm part}$), and $|i\rangle$ is a new state. Having selected the state

$$|\Psi_J\rangle = \sum_{k, i_{\rm prev}, J_{\rm part}, i} c^{(J_{\rm part})}_{k i_{\rm prev} i} [(|k i_{\rm prev}\rangle)^{J_{\rm part}} |i\rangle]^J \qquad (1)$$

with the largest overlap with the vector $|\Psi_J\rangle^{(0)}$ in the pole approximation, one constructs the density matrix

$$\rho^B_{ii';j_B} = \sum_{k, i_{\rm prev}, J_{\rm part}} c^{(J_{\rm part}, j_B)}_{k i_{\rm prev} i} c^{(J_{\rm part}, j_B)}_{k i_{\rm prev} i'} \qquad (2)$$

and keeps $N_{\rm opt}$ eigenvectors $|\alpha\rangle$ with the largest absolute values of eigenvalues. The procedure continues by adding the $(m-1)$st pair of shells, etc., until the first pair of p shells in B is reached, ending the first sweep. Then the procedure is reversed again, continuing sweeping within the B subspace until convergence is reached.

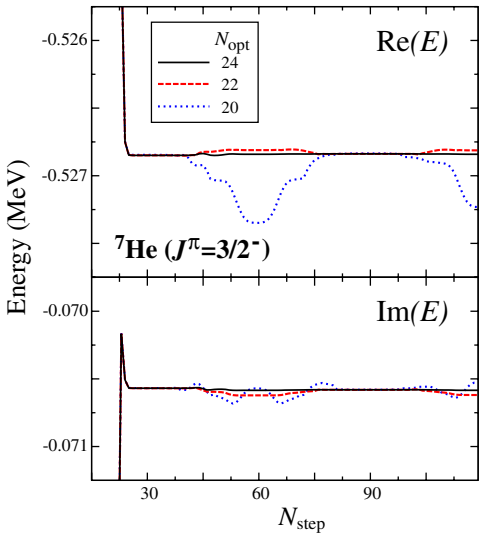

FIG. 1 (color online). GSM + DMRG results for the real (top panel) and imaginary (bottom panel) parts of the g.s. ($J^\pi = 3/2^-$) energy of ^{7}He plotted as a function of the number of DMRG steps. The number of states kept during the sweeping phase is $N_{opt} = 20$ (dotted lines), 22 (dashed lines), and 24 (solid lines).

In the examples presented in this work, the number of SP shells included in A and B are $N_r = 2$ and $N_c = 60$ (30 shells in each continuum: $\{p_{1/2}\}_c$, $\{p_{3/2}\}_c$), respectively. In the warm-up phase, $N^0_{opt} = 8$; i.e., we keep one vector for each family $\{n; j_B\}$. Figure 1 shows the convergence properties of the ground state (g.s.) $J^\pi = 3/2^-$ resonance energy in ^{7}He plotted as a function of the number of DMRG steps N_{step}. Converged results, manifested by a local plateau at the complex energy $E = E_0$, are found after $N_{step} \leq 30$ steps. Then, with increasing N_{step}, one enters the unstable region ($40 \leq N \leq 70$). A second plateau, corresponding to practically the same energy E_0 as the first plateau (and fairly independent of N_{opt}), appears at $N_{step} \sim 90$. The "plateau-unstable" sequence repeats periodically. It is worth noting that the deviation from Re(E_0) can be both positive and negative. This is because the GSM Hamiltonian matrix is not Hermitian but complex symmetric; hence, the usual reasoning based on the Ritz variational principle does not apply.

The behavior of the DMRG procedure, as can be seen in Fig. 1 and Table I, shows a gradual reduction of the energy variation around the plateau with an increasing number of sweeps. Most importantly, the variation decreases quickly with the number of states N_{opt} kept in the sweeping phase. The relative precision of the DMRG procedure is extremely high: $\sim 10^{-6}$ for $N_{opt} = 24$ and $N_{sw} = 4$.

Figure 2 illustrates the convergence of the DMRG procedure for the first excited state in ^{7}He, which is calculated to be a broad resonance with $\Gamma = 3.37$ MeV. Here, 7 vectors are kept in the warm-up phase. The full convergence is attained in about 2 sweeps; i.e., the procedure is somewhat slower than for the narrow g.s. resonance ($\Gamma = 0.14$ MeV). Still, the resulting plateau is excellent. Again, as in Fig. 1, E_0 is practically independent of N_{opt}. These two examples demonstrate that the proposed DMRG algorithm is extremely efficient in optimizing SP nonresonant space.

TABLE I. Relative DMRG precision $\Delta E/E$ of the real part of the g.s. energy in ^{7}He as a function of the number of states N_{opt} kept in the sweeping phase at the second ($N_{sw} = 2$) and fourth ($N_{sw} = 4$) sweep. ΔE is a difference of the extremal values of the real part of the g.s. energy during a sweep, and $E = \mathrm{Re}(E_0)$ is the exact value.

N_{opt}	$\Delta E/E$ ($N_{sw} = 2$)	$\Delta E/E$ ($N_{sw} = 4$)
20	9.4×10^{-4}	7.5×10^{-4}
22	8.0×10^{-5}	4.9×10^{-5}
24	3.0×10^{-5}	4.7×10^{-6}
26	2.1×10^{-5}	2.6×10^{-6}

A major problem in studies of OQS is to maintain the completeness of the many-body basis containing contributions from *discretized* nonresonant SP continua. In this respect, the Berggren ensemble is not different. The accuracy of GSM calculations relies upon the independence of calculated observables such as energies, transition probabilities, and cross sections on the number of SP shells in the complex nonresonant continuum. To illustrate this point, we show in Fig. 3 the g.s. energy of ^{7}He as a function of the total number of SP shells N_{sh}. One can see that the dependence of Re(E) and Im(E) on N_{sh} is not monotonic, showing oscillations which disappear only if a sufficiently dense

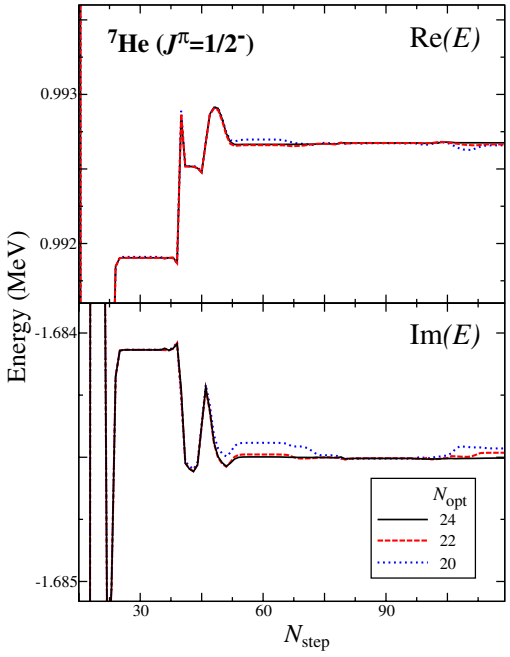

FIG. 2 (color online). Similar to Fig. 1 except for the first excited state ($J^\pi = 1/2^-$) in ^{7}He.

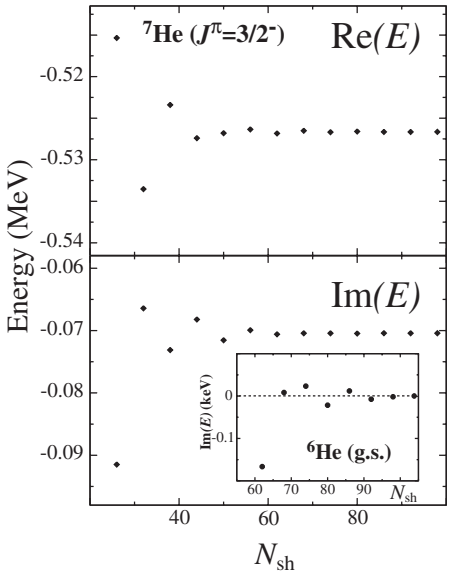

FIG. 3. Convergence of the real (top panel) and imaginary (bottom panel) parts of the g.s. energy of ^{7}He as a function of the total number of shells $N_{sh}(\equiv N_c + N_r = N_c + 2)$ included in the SP basis. As in Fig. 1, 8 vectors are kept in the warm-up phase. In the sweeping phase, $N_{opt} = 22$ states are kept. The inset shows the imaginary part of the g.s. energy of ^{6}He as a function of N_{sh}. Here, $N_{opt} = 4$ (10) vectors were kept in the warm-up (sweeping) phase.

discretization is applied. A similar oscillatory pattern is seen in the imaginary part of the g.s. energy of ^{6}He (shown in the inset). Since ^{6}He is bound, the deviation of Im(E) from zero is due to too coarse a discretization; the completeness is practically achieved for $N_{sh} = 70$. While the error due to an insufficient number of nonresonant shells is of the order of 10^{-2} keV, the accuracy of DMRG is in the range of 10^{-6} keV.

The results shown in Figs. 1–3 demonstrate that the fully converged GSM results, with respect to both the number of sweeps and the number of shells in the discretized continua, can be obtained using the GSM + DMRG algorithm. The rank of the biggest matrix to be diagonalized in GSM + DMRG is practically constant with respect to N_{sh}. In the example shown in Fig. 3, it changes from $d = 941$ to $d = 1001$, whereas the dimension of the GSM matrix in the J-coupling scheme varies as $D \propto N_{sh}^3$, from $D = 6149$ for $N_{sh} = 26$, to $D = 332\,171$ for $N_{sh} = 98$. Hence, the gain factor $D(N_c)/d(N_c) \sim N_{sh}^3$ quickly grows with increasing N_c (or the size of block B). Our results indicate that (i) the complex energy E_0 at the DMRG plateau very weakly depends on N_{opt}, and (ii) the precision of calculated complex energies weakly depends on N_{sh}, provided that N_{sh} is sufficiently large. This means that the convergence features of the GSM + DMRG procedure can be tested by varying N_{sh} and N_{opt}. Once those parameters are optimized in "small-scale" GSM + DMRG calculations, the final calculations can be performed in the large model space to obtain fully converged results.

In summary, this study describes the first application of the DMRG method to unbound many-fermion systems described by a complex-symmetric eigenvalue problem. The encouraging features of the proposed GSM + DMRG approach make it the tool of choice for studies of the continuum effects in multiparticle OQS such as open microwave resonators, multielectron open quantum dots, atomic nuclei, and atomic clusters close to the particle drip line.

This work was supported by the U.S. Department of Energy under Contracts No. DE-FG02-96ER40963 (University of Tennessee), No. DE-AC05-00OR22725 with UT-Battelle, LLC (Oak Ridge National Laboratory), and No. DE-FG05-87ER40361 (Joint Institute for Heavy Ion Research), and by the Spanish DGI under Grant No. BFM2003-05316-c02-02.

[1] T. Berggren, Nucl. Phys. **A109**, 265 (1968); T. Berggren and P. Lind, Phys. Rev. C **47**, 768 (1993).
[2] N. Michel *et al.*, Phys. Rev. Lett. **89**, 042502 (2002); N. Michel *et al.*, Phys. Rev. C **67**, 054311 (2003).
[3] R. Id Betan *et al.*, Phys. Rev. Lett. **89**, 042501 (2002).
[4] J. Humblet and L. Rosenfeld, Nucl. Phys. **26**, 529 (1961).
[5] N. Michel, W. Nazarewicz, and M. Płoszajczak, Phys. Rev. C **70**, 064313 (2004).
[6] M. Barranco, J. Navarro, and A. Poves, Phys. Rev. Lett. **78**, 4729 (1997); R. Guardiola and J. Navarro, Phys. Rev. Lett. **84**, 1144 (2000).
[7] S. R. White, Phys. Rev. Lett. **69**, 2863 (1992); Phys. Rev. B **48**, 10 345 (1993).
[8] J. Dukelsky and S. Pittel, Rep. Prog. Phys. **67**, 513 (2004).
[9] U. Schollwöck, Rev. Mod. Phys. **77**, 259 (2005).
[10] S. R. White and R. L. Martin, J. Chem. Phys. **110**, 4127 (1999).
[11] J. Dukelsky and G. Sierra, Phys. Rev. Lett. **83**, 172 (1999).
[12] N. Shibata and D. Yoshioka, Phys. Rev. Lett. **86**, 5755 (2001).
[13] J. Dukelsky *et al.*, Phys. Rev. C **65**, 054319 (2002).
[14] E. Carlon, M. Henkel, and U. Schollwöck, Eur. Phys. J. B **12**, 99 (1999).
[15] T. Papenbrock and D. J. Dean, J. Phys. G **31**, S1377 (2005).
[16] S. Pittel and N. Sandulescu, Phys. Rev. C **73**, 014301 (2006).
[17] N. Michel *et al.*, Rev. Mex. Fis. **50**, 74 (2004).
[18] This selection rule for many-body resonant states is unique to GSM + DMRG: in standard DMRG approaches, the lowest-energy eigenvalue in the superblock Hamiltonian is selected.
[19] I. McCulloch and M. Gulacsi, Europhys. Lett. **57**, 852 (2002).
[20] ρ^B is block diagonal in j_B and complex symmetric. Hence, its eigenvalues are complex.